

IFUSP/P-62

RESONANT RAMAN SCATTERING BY LO PHONONS IN THE
PRESENCE OF A STATIC MAGNETIC FIELD *

SONIA FROTA-PESSOA **

Instituto de Física, Universidade de São Paulo,
C.P. 20516, São Paulo, S.P., Brazil

and

ROBERTO LUZZI

Instituto de Física "Gleb Wataghin", Universidade
Estadual de Campinas, 13.100, Campinas, S.P.,
Brazil.

B.I.F. - USP

* Supported in part by BID, BNDE, FNDCT and CNPq.

** Paper based on a thesis submitted by one of the authors (S.F.P.)
in partial fulfillment of Ph.D. degree in the Instituto de Física
"Gleb Wataghin", Universidade Estadual de Campinas, Campinas,
S.P., Brazil.

To be published in PHYSICAL REVIEW B

RESONANT RAMAN SCATTERING BY LO PHONONS IN THE PRESENCE
OF A STATIC MAGNETIC FIELD *

Sonia Frota-Pessoa **

Instituto de Física, Universidade de São Paulo
C.P. 20516, São Paulo, S.P., Brazil

and

Roberto Luzzi

Instituto de Física "Gleb Wataghin", Universidade Estadual de
Campinas, 13.100, Campinas, S.P., Brazil

ABSTRACT

Resonant Raman scattering from LO phonons in the presence of a constant magnetic field is considered. We calculate the differential extinction coefficient, including effects of the electron-phonon interaction, for a doped semiconductor. It is shown that significant deviations from the Lorentzian lineshape may appear due to hybridization of the phonon mode with the cyclotron modes, when for certain geometries, a harmonic of the cyclotron frequency is approximately equal to the LO phonon frequency. An application is made for GaAs.

* Supported in part by BID, BNDE, FNDCT and CNPq.

** Paper based on a thesis submitted by one of the authors (S.F.P.) in partial fulfillment of Ph.D. degree in the Instituto de Física "Gleb Wataghin", Universidade Estadual de Campinas, Campinas, S.P., Brazil.

I - INTRODUCTION

Inelastic scattering of light has proved to be a useful tool to study hybridization of elementary excitations in semiconductors, e.g. hybrid phonon-photon (1), plasmon-phonon (2), plasmon-polariton (3), different symmetry phonons (4), and other coupled excitations. Raman scattering of light by crystals in the presence of a constant magnetic field has been considered by several authors, who studied scattering either by Landau levels, more precisely, by Bernstein modes (5), or by the coupled electron-phonon system (6,7). As shown by Wolff (5), electrons in a nearly parabolic conduction band, do not scatter light in the dipole approximation. However, in n-type semiconductors having a non-parabolic conduction band, a small forbidden energy gap and a small conduction band effective mass, the scattering cross section is finite and should be detectable experimentally. This magneto-Raman scattering was later observed in InSb and InAs (8). These experiments showed deviations from the behavior predicted (5) for the Raman frequency shift at energies close to the LO phonon frequency. These deviations were ascribed to polaron effects, i.e. electron-phonon mixing (7). In these experiments, the Raman line is composed almost exclusively of the electron-like contribution to the hybrid modes (7).

In the case of parabolic band semiconductors, on the contrary, the electron-like contribution to the Raman line is negligible when compared to the phonon-like contribution (9). Genkin and Zil'berberg (6) have pointed out the possibility of

resonant Raman scattering by LO phonons when the phonon frequency equals a harmonic of the cyclotron frequency. An additional enhancement of the LO phonon Raman line can be observed in highly photo-excited semiconductors ⁽¹¹⁾. This enhancement is assumed to be due to a LO phonon distribution strongly departed from equilibrium, which results when injected photoelectrons cascade down the Landau-levels with the emission of LO phonons. Raman scattering experiments can be a very convenient way to study the LO phonon-Landau level system in conditions of approximate statistical equilibrium or in the presence of hot excitations.

We present here a study of inelastic scattering of light, in a static magnetic field, by the coupled electron-phonon system in a direct gap, n-type semiconductor with a parabolic conduction band. We consider the effect of the electron-phonon interaction on the scattering amplitude and on the line shape. Significant effects appear in these quantities due to the quantization of the electron states in a magnetic field. Neglecting the lifetime of the virtual electron states, the scattering amplitude shows singularities of a logarithmic nature. This fact, together with the effect of the frequency dependence of the phonon damping produces a Raman spectrum possessing a complex structure.

II. DIFFERENTIAL EXTINCTION COEFFICIENT

We consider a monochromatic beam of photons from a laser source of frequency ω_2 , incident on an n-type semiconductor crystal. The Hamiltonian of the system is given by

$$H = H_E + H_L + H_{EL} + H_R + H_{ER} \quad (1)$$

where H_E is the Hamiltonian for the many electron system, H_L is that of the phonon system, H_{EL} represents the electron-phonon interaction energy, H_R is the Hamiltonian of the radiation field and H_{ER} is the interaction between the radiation and the electron system. We assume the crystal to be in the presence of a static magnetic field \vec{H} , with the associated vector potential given in the Landau gauge $\vec{A}_0 = (-yH, 0, 0)$.

We neglect the deformation potential contribution to the electron-phonon interaction energy since, in the case of polar crystals, it is generally negligible when compared with the long-range electrostatic interaction between electrons and longitudinal optical phonons. Therefore the electron-phonon interaction will be described in this case by the Fröhlich Hamiltonian (12). We work within the effective mass approximation and take the one-electron wave functions to be the Landau functions (13) $|n, k_x, k_z, \sigma\rangle$, where n is the Landau level quantum number and σ the spin quantum number. The corresponding one electron energies are $E_n(k_z) = (n + 1/2)h\omega_c + \hbar^2 k_z^2 / 2m^*$, where $\omega_c = (eH/m^*c)$ is the cyclotron frequency of the conduction band electrons.

In Figure 1, we show the Raman processes which give rise to scattering by LO phonons. The diagram (a) involves the A^2 part of H_{ER} , where \vec{A} is the vector potential of the radiation field and which, here, connects intraband electronic states. The diagram (b) involves the $\vec{A} \cdot \vec{p}$ part of H_{ER} twice, which, for the resonant condition, $\omega_0 \approx n\omega_c$, connects interband electronic states.

In absence of the static magnetic field, the contribution to the differential extinction coefficient comes from the type (b) diagram. In the present situation however, the first process (a) is resonant and, in some materials, may dominate over type (b). In the following discussion we assume this to be the case, and consider only contributions from diagram (a).

We consider the anti-Stokes Raman process in which inelastic scattering of photons results in the production of a phonon with the virtual participation of the electrons. In our present treatment we neglect temperature effects since a finite temperature will broaden the Raman line and may wash out the effects resulting from phonon hybridization in which we are interested.

The scattering Hamiltonian is taken to be $H = H_{EL} + H_{ER}$ which connects the specified initial and final states only in second order of perturbation theory. To obtain the differential extinction coefficient it is necessary to calculate the transition probability between the specified initial and final states. For this purpose, we evaluate the second order contribution to the S-matrix expansion

$$S^{(2)} = \frac{(-i/\hbar)^2}{2!} \iint dt dt' P \{ V_{EL}(t) V_{ER}(t') + V_{ER}(t) V_{EL}(t') \} \quad (2)$$

where

$$V_{ER}(t) = \sum_{\vec{k}_\lambda, \vec{k}_\mu} \sum_{n, \vec{k}} \sum_{n', \vec{k}'} A_{\lambda\mu} \langle n', \vec{k}' | e^{i(\vec{k}_\lambda - \vec{k}_\mu) \cdot \vec{r}} | n, \vec{k} \rangle a^\dagger(\vec{k}_\mu, t) \\ \times a(\vec{k}_\lambda, t) c_{n', \vec{k}'}^\dagger(t) c_{n\vec{k}}(t) \quad (3)$$

$$V_{EL}(t) = \sum_{\vec{n}\vec{k}} \sum_{\vec{n}'\vec{k}'} \sum_{\vec{q}} V_q \langle \vec{n}', \vec{k}' | e^{i\vec{q} \cdot \vec{r}} | \vec{n}, \vec{k} \rangle c_{\vec{n}'\vec{k}'}^\dagger(t) c_{\vec{n}\vec{k}}(t) b_{\vec{q}}^\dagger(t) \quad (4)$$

are the relevant parts of H_{ER} and H_{EL} respectively for the process (a) in Figure 1.

In Eq. (3) and (4) we have introduced

$$A_{\lambda\mu} = \frac{2\pi\hbar e^2}{vm^*c} \frac{(\hat{e}_\lambda \cdot \hat{e}_\mu)}{\epsilon_\infty^{1/2} \sqrt{k_\lambda k_\mu}} \quad (5)$$

and

$$V_q = i \frac{e}{q} \left(\frac{2\pi\hbar}{v} \right)^{1/2} \omega_0^{1/2} (\epsilon_\infty^{-1} - \epsilon_0^{-1})^{1/2} \quad (6)$$

We have simplified our notation for the Landau functions to either, $|\vec{n}, \vec{k}\rangle$ or $\phi_{\vec{n}\vec{k}}(\vec{r})$. The radiation polarization vector are $\hat{e}_\lambda, \hat{e}_\mu$. v is the volume of the system and ω_0 the LO phonon frequency (dispersion has been neglected) and $c_{\vec{n}, \vec{k}}, b_{\vec{q}}$ and $a(\vec{k}_\mu)$ are second quantization operators for electrons, phonons and photons respectively. Finally P is Dyson's time ordering operator, which, in the present case, can be replaced by Wick's time ordering operator T without alteration. To include effects of mode hybridization we assume the asymptotic states to consist of free photon states and interacting electron and phonon states. We neglect the electron lifetimes and use Wick's theorem to find, for the relevant matrix elements of $S^{(2)}$,

$$\begin{aligned} \langle f | S^{(2)} | i \rangle = & \sum_{\vec{q}} \frac{A_{LR} V_q \sqrt{n_L}}{\hbar^2} \int d^3r dt \int d^3r' dt' e^{-i(\omega_L - \omega_R)t} e^{-i(\vec{k}_L - \vec{k}_R) \cdot \vec{r}} \\ & \times e^{-i\vec{q} \cdot \vec{r}'} \langle f^* | b_{\vec{q}}^\dagger(t') | i^* \rangle \langle i^* | T \{ \psi^\dagger(\vec{r}, t) \psi(\vec{r}, t) \psi^\dagger(\vec{r}', t') \psi(\vec{r}', t') \} | i^* \rangle \end{aligned} \quad (7)$$

where

$$\psi(\vec{r}, t) = \sum_{n\vec{k}} \phi_{n\vec{k}}(\vec{r}) c_{n\vec{k}}(t) \quad (8)$$

and $|i^*\rangle$, $|f^*\rangle$ are the initial and final crystal states. Here we also have:

$$\begin{aligned} \langle i^* | T \{ \psi^\dagger(\vec{r}, t) \psi(\vec{r}, t) \psi^\dagger(\vec{r}', t') \psi(\vec{r}', t') \} | i^* \rangle = \\ = - G^0(\vec{r}t, \vec{r}t') G^0(\vec{r}'t', \vec{r}'t') + G^0(\vec{r}t, \vec{r}'t') G^0(\vec{r}'t', \vec{r}t) \end{aligned} \quad (9)$$

where

$$G^0(\vec{r}t, \vec{r}'t') = -i \langle \phi_0 | T \{ \psi(\vec{r}, t) \psi^\dagger(\vec{r}', t') \} | \phi_0 \rangle \quad (10)$$

is the one electron zero temperature Green's function ⁽¹⁴⁾ in the presence of a magnetic field, and $|\phi_0\rangle$ is the ground state for the electronic system. We find:

$$\begin{aligned} G^0(\vec{r}t, \vec{r}'t') = \sum_{n\vec{k}} \phi_{n\vec{k}}(\vec{r}) \phi_{n, \vec{k}}^*(\vec{r}') \int_{-\infty}^{\infty} \frac{d\omega}{2\pi} e^{i\omega(t-t')} \\ \times \left\{ \frac{\theta(|k_z| - k_{zF}^{(n)})}{\omega - \omega_n(k_z) + is} + \frac{\theta(k_{zF}^{(n)} - |k_z|)}{\omega - \omega_n(k_z) - is} \right\} \end{aligned} \quad (11)$$

where

$$\omega_n(k_z) = \hbar^{-1} E_n(k_z),$$

$$k_{zF}^{(n)} = \left| \left\{ \mu - (n+1/2)\hbar\omega_c \right\} 2m^*/\hbar^2 \right|^{1/2}$$

and

$$k_{zF}^{(n)} = 0 \quad \text{if} \quad n > n_0$$

μ being the chemical potential which coincides here with the Fermi energy of the electron gas and $\theta(x)$ the step function. The first term on the right hand side of Eq.(9) vanishes in our case and Eq. (7) becomes

$$\begin{aligned} \langle f | S^{(2)} | i \rangle &= \sum_{n\vec{k}} \sum_{n'\vec{k}'} \sum_{\vec{q}} \pi^{-2} A_{LR} V_q \sqrt{n_L} \langle n, \vec{k} | e^{i(\vec{k}_L - \vec{k}_R) \cdot \vec{r}} | n', \vec{k} \rangle \\ &\times \langle n', \vec{k}' | e^{-i\vec{q} \cdot \vec{r}} | n, \vec{k} \rangle \int \frac{d\omega}{2\pi} \int \frac{d\omega'}{2\pi} \int dt \int dt' e^{-i(\omega_L - \omega_R + \omega - \omega')t} \\ &\times e^{i(\omega - \omega')t'} \langle f^* | b_{\vec{q}}^\dagger(t') | i^* \rangle F_{nn'}(k_z, k'_z; \omega, \omega') \end{aligned} \quad (12)$$

where

$$\begin{aligned} F_{nn'}(k_z, k'_z; \omega, \omega') &= \frac{\theta(|k_z| - k_{zF}^{(n)}) \theta(|k'_z| - k_{zF}^{(n')})}{(\omega - \omega_n(k_z) + is)(\omega' - \omega_{n'}(k'_z) + is)} + \\ &+ \frac{\theta(|k_z| - k_{zF}^{(n)}) \theta(k_{zF}^{(n')} - |k'_z|)}{(\omega - \omega_n(k_z) + is)(\omega' - \omega_{n'}(k'_z) - is)} + \frac{\theta(k_{zF}^{(n)} - |k_z|) \theta(|k'_z| - k_{zF}^{(n')})}{(\omega - \omega_n(k_z) - is)(\omega' - \omega_{n'}(k'_z) + is)} + \\ &+ \frac{\theta(k_{zF}^{(n)} - |k_z|) \theta(k_{zF}^{(n')} - |k'_z|)}{(\omega - \omega_n(k_z) - is)(\omega' - \omega_{n'}(k'_z) - is)} \end{aligned} \quad (13)$$

Using

$$\langle n, \vec{k} | e^{i\vec{Q} \cdot \vec{r}} | n', \vec{k}' \rangle = \delta(k'_z, k_z + Q_z) \delta(k'_x, k_x + Q_x) I_{nn'}(k_x, k'_x, \vec{Q}) \quad (14)$$

where

$$I_{nn'}(k_x, k'_x, \vec{Q}) = e^{i \frac{\lambda^2}{2} Q_y (k_x + k'_x)} I_{nn'}(\vec{Q}) \quad (15)$$

and

$$I_{nn'}(\vec{Q}) = 2^{(n'-n)/2} \frac{n!}{n'} \left(\frac{\lambda}{2} (Q_x - iQ_y)\right)^{n'-n} e^{-\frac{\lambda^2}{4} Q_{\perp}^2} L_n^{n'-n}\left(\frac{\lambda^2}{2} Q_{\perp}^2\right) \quad (16)$$

with $Q_{\perp}^2 = Q_x^2 + Q_y^2$, $\lambda^2 = e\hbar/cH$ and $L_n^m(x)$ are the Laguerre Polynomials.

Performing the integrations on ω , ω' and t in Eq.(12), summing over \vec{k}' and k_x and using the resulting $\delta(\vec{q}, \vec{k}_L - \vec{k}_R)$ to sum over \vec{q} we find:

$$\begin{aligned} \langle f | S^{(2)} | i \rangle = & \frac{iA_{RL} V_q \sqrt{n_L}}{2\hbar^2 \pi^2 \lambda^2} \sum_{\ell=1}^{\infty} \sum_{n=0}^{n_0} |I_{n, n+\ell}(q_{\perp})|^2 \int dk_z \\ & \times \left\{ \frac{\theta(|k_z| - k_{zF}^{(n+\ell)}) \theta(k_{zF}^{(n)} - |k_z|)}{\omega - \ell\omega_c - \hbar k_z q_z / m^* + is} - \frac{\theta(|k_z| - k_{zF}^{(n+\ell)}) \theta(k_{zF}^{(n)} - |k_z|)}{\omega + \ell\omega_c - \hbar k_z q_z / m^* - is} \right\} \\ & \times \int dt e^{i\omega t} \langle f^* | b_{\vec{q}}^+(t) | i^* \rangle \quad (17) \end{aligned}$$

where n_0 is the highest non-empty Landau level in the ground state, $\omega = \omega_L - \omega_R$ is the energy transfer and $\vec{q} = \vec{k}_L - \vec{k}_R$ the momentum transfer. We neglect q_z when compared with k_z and let $s \rightarrow 0$ in the energy denominators in order to have a well defined integral over k_z .

We are now in condition to calculate the differential extinction coefficient (15)

$$\frac{d^2 h}{d\Omega d\omega_R} = \frac{P(\Omega, \omega)}{n_L c \epsilon_{\infty}^{-1/2}} \quad (18)$$

Here $P(\Omega, \omega)d\Omega d\omega_R$ is the transition probability rate for a photon with frequency in the interval $\omega_R < \omega < \omega_R + d\omega_R$ to be scattered in a direction $\Omega(\theta, \phi)$ within a solid angle $d\Omega$, i.e.

$$P(\Omega, \omega) = \sum_{f^*} \frac{v}{(2\pi)^3} \frac{\omega_R^2}{c^3 \epsilon_\infty^{-3/2}} \frac{1}{I} \left| \langle f^* | S^{(2)} | i^* \rangle \right|^2, \quad (19)$$

$$I = \lim_{t_0 \rightarrow \infty} \int_{-t_0}^{t_0} dt$$

Substituting Eq. (19) in Eq. (18) we have:

$$\frac{d^2 h}{d\Omega d\omega_R} = \frac{d^2 h}{d\Omega d\omega} \Big|_0 L_{\vec{q}}(\omega) \quad (20)$$

where

$$\begin{aligned} \frac{d^2 h}{d\Omega d\omega} \Big|_0 &= c_q \left| \sum_{\ell=1}^{\infty} \sum_{n=0}^{n_0} |I_{n, n+\ell}(q_{\perp})|^2 \int dk_z \theta(|k_z| - k_{zF}^{(n+\ell)}) \theta(k_{zF}^{(n)} - |k_z|) \right. \\ &\times \left. \left\{ \frac{1}{\omega - \ell\omega_c - \hbar k_z q_z / m^* + is} - \frac{1}{\omega + \ell\omega_c - \hbar k_z q_z / m^* - is} \right\} \right|^2, \quad (21) \end{aligned}$$

$$|I_{nn'}(q_{\perp})|^2 = \frac{n!}{n'!} \left(\frac{\lambda^2 q_{\perp}^2}{2}\right)^{n'-n} e^{-\frac{\lambda^2}{2} q_{\perp}^2} \left| L_n^{n'-n} \left(\frac{\lambda^2}{2} q_{\perp}^2\right) \right|^2, \quad (22)$$

$$c_q = \frac{e^6 \omega_0 (\hat{e}_R \cdot \hat{e}_L)^2}{2c^4 m^{*2} q^2 \pi^3 \hbar \lambda^4} (\epsilon_\infty^{-1} - \epsilon_0^{-1}), \quad (23)$$

and

$$L_{\vec{q}}^{\uparrow}(\omega) = \frac{1}{T} \sum_{f^*} \left| \int_{-\infty}^{\infty} \frac{e^{-i\omega t}}{\sqrt{2\pi}} \langle f^* | b_{\vec{q}}^{\uparrow}(t) | i^* \rangle \right|^2 \quad (24)$$

It is convenient to express Eq.(24) in terms of the spectral density and phonon Green's function. We can rewrite Eq.(24) as

$$\begin{aligned} L_{\vec{q}}^{\uparrow}(\omega) &= \frac{1}{T} \int_{-\infty}^{\infty} dt \int_{-\infty}^{\infty} dt' \frac{e^{-i\omega(t'-t)}}{2\pi} \sum_{f^*} \langle i^* | b_{\vec{q}}^{\uparrow}(t) | f^* \rangle \langle f^* | b_{\vec{q}}^{\uparrow}(t') | i^* \rangle = \\ &= \int_{-\infty}^{\infty} d\tau \frac{e^{i\omega\tau}}{2\pi} \langle b_{\vec{q}}^{\uparrow}(\tau) b_{\vec{q}}^{\uparrow}(0) \rangle \end{aligned} \quad (25)$$

where $\langle \dots \rangle$ stands for the statistical average value.

Within the above mentioned limitations we have obtained an analog of van Hove's result (16), and, therefore, the Green's function formalism, as described in the already classical paper by Zubarev (17), can be used to obtain:

$$\frac{d^2 h}{d\Omega d\omega_R} = \frac{d^2 h}{d\Omega d\omega} \Big|_0 \frac{1}{\pi} \text{Im } G_{\vec{q}}^{\uparrow}(\omega+is) \quad (26)$$

where

$$G_{\vec{q}}^{\uparrow}(\omega+is) = \langle\langle b_{\vec{q}}^{\uparrow} | b_{\vec{q}}^{\uparrow} ; \omega+is \rangle\rangle \quad (27)$$

is the phonon Green's function.

We refer to the first factor in Eq. (26) as the scattering strength, even though it is frequency dependent, and to the second factor as the line shape.

If the phonon states are truly stationary the crystal state

$|r^*\rangle$ can be written as a product of electron and phonon states and the line shape reduces to the energy conserving function $\delta(\omega - \omega_0)$.

III. THE LINE SHAPE

Next we proceed to evaluate the one phonon Green's function including Fröhlich interaction. Using the standard decoupling procedures (17) we find, including terms up to second order in the electron phonon interaction,

$$G_{\vec{q}}(\omega + is) = (\omega - \omega_0 - P_{\vec{q}}(\omega + is))^{-1} \quad (28)$$

where

$$P_{\vec{q}}(\omega + is) = P_{\vec{q}}(\omega) - i \gamma_{\vec{q}}(\omega) \quad (29)$$

$$P_{\vec{q}}(\omega) = P \sum_{n', n, \vec{k}} \hbar^{-1} |V_{\vec{q}} I_{n, n'}(q_{\perp})|^2 \frac{\{ f(n, \vec{k} - \vec{q}) - f(n', \vec{k}) \}}{\hbar\omega - \epsilon_{n'}(k_z) + \epsilon_n(k_z - q_z)} \quad (30)$$

$$\gamma_{\vec{q}}(\omega) = \pi \hbar^{-2} \sum_{n', n, \vec{k}} |V_{\vec{q}} I_{n, n'}(q_{\perp})|^2 \{ f(n, \vec{k} - \vec{q}) - f(n', \vec{k}) \} \cdot \delta(\hbar^{-1}(\hbar\omega - \epsilon_{n'}(k_z) + \epsilon_n(k_z - q_z))) \quad (31)$$

Here $f(n, \vec{k})$ is the Fermi-Dirac distribution function and $\epsilon_n(k_z) = \hbar\omega_c(n+1/2) + \hbar^2 k_z^2 / 2m^* - \mu$, μ being the chemical potential and p.v. stands for principal value. We will consider the case of concentrations n_e such that the dependence of the chemical po-

tential on the magnetic field can be neglected so that $\mu = (\hbar/2m^*) (3\pi^2 n_e)^{2/3}$. After some computational work we find:

$$P_{\vec{q}}(\omega) = \sum_{\ell=1}^{\infty} \sum_{n=0}^{n_0} \frac{D(q_{\perp}, q_z)}{\pi} \frac{\rho^{\ell-1} (n+\ell)!}{(\ell!)^2 n!} \left\{ \ell n \left| \frac{\omega^2 - (\ell\omega_c - \beta^{(n)})^2}{\omega^2 - (\ell\omega_c + \beta^{(n)})^2} \right| + \right. \\ \left. + \ell n \left| \frac{\omega^2 - (\ell\omega_c + \beta^{(n+\ell)})^2}{\omega^2 - (\ell\omega_c - \beta^{(n+\ell)})^2} \right| \right\} \quad (32)$$

and

$$\gamma_{\vec{q}}(\omega) = \sum_{\ell=1}^{\infty} \sum_{n=0}^{n_0} \gamma_{n,\ell}(\omega) \quad (33)$$

where

$$\gamma_{n,\ell}(\omega) = D(q_{\perp}, q_z) \frac{\rho^{\ell-1} (n+\ell)!}{(\ell!)^2 n!} \quad \text{if } \beta^{(n+\ell)} < |\omega - \ell\omega_c| < \beta^{(n)} \quad (34)$$

and ZERO otherwise.

In equations (32) and (34) we have introduced, $\rho = \frac{\lambda^2}{2} q_{\perp}^2$, $\beta^{(n)} = \hbar q_z k_{zF}^{(n)} / m^*$ and $D(q_{\perp}, q_z) = \frac{e^2 m^* \omega_0 q_{\perp}^2}{2\hbar^2 q_z (q_{\perp}^2 + q_z^2)} (\epsilon_{\infty}^{-1} - \epsilon_0^{-1})$. In

deriving $P_{\vec{q}}(\omega)$ and $\gamma_{\vec{q}}(\omega)$ we have used the fact that \vec{q} (the photon momentum transfer) is very small and one can assume $\rho \ll 1$ and $q_z \ll k_{zF}^{(n)}$. Blank and Kaner (18) derived expressions for $P_{\vec{q}}(\omega)$ and $\gamma_{\vec{q}}(\omega)$ for acoustic phonons interacting with cyclotron modes. In their calculation the leading contributions are due to electronic intralevel transitions, whereas in our calculations, involving low momentum optical phonons, electronic inter-level transitions are the most important contributions.

To end this section we should point out that, in terms of the real and imaginary parts of polarization operator $P_{\vec{q}}(\omega)$, the line shape given in Eq.(26) can be written as:

$$L_{\vec{q}}(\omega) = \frac{1}{\pi} \text{Im } G_{\vec{q}}(\omega + i\epsilon) = \frac{1}{\pi} \frac{\gamma_{\vec{q}}(\omega)}{|\omega - \omega_0 - P_{\vec{q}}(\omega)|^2 + (\gamma_{\vec{q}}(\omega))^2} \quad (35)$$

IV- THE SCATTERING STRENGTH

We evaluate the scattering strength $\left. \frac{d^2h}{d\Omega d\omega} \right|_0$ as given in Eq. (21), introducing, however, electron lifetimes in a phenomenological way (19). We obtain:

$$\left. \frac{d^2h}{d\Omega d\omega} \right|_0 = C_q |N'(\omega) + iN''(\omega)|^2 \quad (36)$$

where

$$N'(\omega) = \sum_{\ell=1}^{\infty} \sum_{n=0}^{n_0} |I_{n,n+\ell}(q_{\perp})|^2 \int_{-\infty}^{\infty} dk_z \theta(|k_z| - k_{zF}^{(n+\ell)}) \theta(k_{zF}^{(n)} - |k_z|) \\ \times \left\{ \frac{\omega - \ell\omega_c - \hbar k_z q_z / m^*}{(\omega - \ell\omega_c - \hbar k_z q_z / m^*)^2 + (\Gamma_{n,n+\ell})^2} - \frac{\omega + \ell\omega_c - \hbar k_z q_z / m^*}{(\omega + \ell\omega_c - \hbar k_z q_z / m^*)^2 + (\Gamma_{n,n+\ell})^2} \right\} \quad (37)$$

and

$$N''(\omega) = -\sum_{\ell=1}^{\infty} \sum_{n=0}^{n_0} |I_{n,n+\ell}(q) |^2 \int_{-\infty}^{\infty} dk_z \theta(|k_z| - k_{zF}^{(n+\ell)}) \theta(k_{zF}^{(n)} - |k_z|) \\ \times \left\{ \frac{\Gamma_{n,n+\ell}}{(\omega - \ell\omega_c - \hbar k_z q_z / m^*)^2 + (\Gamma_{n,n+\ell})^2} + \frac{\Gamma_{n,n+\ell}}{(\omega + \ell\omega_c - \hbar k_z q_z / m^*)^2 + (\Gamma_{n,n+\ell})^2} \right\} \quad (38)$$

Here $\Gamma_{n,n+\ell} = \frac{1}{2} \left(\frac{1}{\tau_n} + \frac{1}{\tau_{n+\ell}} \right)$, with τ_n and $\tau_{n+\ell}$ being the lifetimes of the corresponding Landau one electron states. Clearly Eq.(21) shows resonant denominators when ω approaches a multiple of the cyclotron frequency $\ell\omega_c$, however the finite lifetime of

electron states in Eq.(35) removes the divergence.

Again with $\rho \ll 1$ and $q_z \ll k_{zF}$ we find:

$$\begin{aligned}
 N'(\omega) = & \sum_{\ell=1}^{\infty} \sum_{n=0}^{n_0} \frac{m^* \rho^\ell (n+\ell)!}{2\hbar q_z (\ell!)^2 n!} \left\{ \ell n \left| \frac{(\omega - \ell \omega_c + \beta^{(n)})^2 + (\Gamma_{n,n+\ell})^2}{(\omega - \ell \omega_c + \beta^{(n)})^2 + (\Gamma_{n,n+\ell})^2} \right| + \right. \\
 & + \ell n \left| \frac{(\omega - \ell \omega_c - \beta^{(n+\ell)})^2 + (\Gamma_{n,n+\ell})^2}{(\omega - \ell \omega_c + \beta^{(n+\ell)})^2 + (\Gamma_{n,n+\ell})^2} \right| - \ell n \left| \frac{(\omega + \ell \omega_c + \beta^{(n)})^2 + (\Gamma_{n,n+\ell})^2}{(\omega + \ell \omega_c - \beta^{(n)})^2 + (\Gamma_{n,n+\ell})^2} \right| - \\
 & \left. - \ell n \left| \frac{(\omega + \ell \omega_c - \beta^{(n+\ell)})^2 + (\Gamma_{n,n+\ell})^2}{(\omega + \ell \omega_c + \beta^{(n+\ell)})^2 + (\Gamma_{n,n+\ell})^2} \right| \right\} \quad (39)
 \end{aligned}$$

and

$$N''(\omega) = \sum_{\ell=1}^{\infty} \sum_{n=0}^{n_0} \frac{m^* \rho^\ell (n+\ell)!}{\hbar q_z (\ell!)^2 n!} \{ Z_{\ell,n}^{(-)}(\beta^{(n+\ell)}) - Z_{\ell,n}^{(-)}(\beta^{(n)}) + Z_{\ell,n}^{(+)}(\beta^{(n+\ell)}) - Z_{\ell,n}^{(+)}(\beta^{(n)}) \} \quad (40)$$

where

$$Z_{\ell,n}^{(\pm)}(\beta) = \begin{cases} \arctan \frac{2 \Gamma_{n,n+\ell} \beta}{(\Gamma_{n,n+\ell})^2 + (\omega \pm \ell \omega_c)^2 - \beta^2} & \text{if } \beta^2 - (\omega \pm \ell \omega_c)^2 < (\Gamma_{n,n+\ell})^2 \\ \pi + \arctan \frac{2 \Gamma_{n,n+\ell} \beta}{(\Gamma_{n,n+\ell})^2 + (\omega \pm \ell \omega_c)^2 - \beta^2} & \text{if } \beta^2 - (\omega \pm \ell \omega_c)^2 > (\Gamma_{n,n+\ell})^2 \end{cases} \quad (41)$$

In the next section we present numerical results appropriate for the case of n-type GaAs.

V - RESULTS FOR GaAs

We proceed to apply our results to GaAs. This material was chosen because it has a nearly parabolic conduction band and, therefore, the electronic contribution to the Raman spectrum, through processes suggested by Wolff (5) should be small. On the other hand, for certain experimental geometries, there should exist a Raman spectrum which arises from scattering of light by phonons mainly through process (a) of Fig. 1, and which should be strong enough to be observed experimentally.

In this material the resonant condition $n\omega_c \approx \omega_0$ occurs at values of $H = 217/n$ kOe. In our numerical calculations we consider static magnetic fields of the order of 110 kOe, such that $\omega_0 \approx 2\omega_c$. We consider a carrier concentration of $n_e = 5.7 \times 10^{17} \text{ cm}^{-3}$ which leads to $n_0 = 1$ and a Fermi energy $\mu = 5.9 \times 10^{-14}$ ergs. We consider the $\lambda_L = 10150 \text{ \AA}$, Y.A.G. line which produces a maximum q value of roughly $4 \times 10^5 \text{ cm}^{-1}$. We arbitrarily choose a geometry such that $q = 2 \times 10^5 \text{ cm}^{-1}$. In the calculations we used the following values for the parameters of GaAs: $m^* = 0.068 m_0$, $\epsilon_\infty = 10.9$, $\epsilon_0 = 12.9$, $\omega_0 = 5.6 \times 10^{13} \text{ seg}^{-1}$ and $\epsilon_g = 2.43 \times 10^{-12}$ ergs. One should note that the Raman intensity is proportional to $|\hat{e}_L \cdot \hat{e}_R|^2$, but the most interesting angular dependence is related to the orientations of the phonon momentum with respect to the direction of the static magnetic field. For fixed $|\vec{q}|$, the angle ϕ between the phonon momentum \vec{q} and \vec{H} determines the magnitudes of q_z and q_\perp which, as we have seen from the calculations, are very important parameters. In what follows, we have fixed $|\vec{q}|$ and varied the direction of \vec{H} , changing the angle ϕ in the calculations.

In Fig. 2, we show $P_{\vec{q}}(\omega)$ and $\gamma_{\vec{q}}(\omega)$ related, respectively,

to the real and imaginary parts of the polarization operator $P_{\vec{q}}(\omega)$ in Eq. (29). We note that only the $\ell = 2$ term in Eq. (33) contributes to the imaginary part $\gamma_{\vec{q}}(\omega)$ in the frequency region $\omega \approx 2\omega_c$, but there can be strong non-resonant contributions to the real part $P_{\vec{q}}(\omega)$ in this frequency range. In Fig. 2, we plot not only $P_{\vec{q}}(\omega)$, but also $P_{\vec{q}}^R(\omega)$, the $\ell = 2$ resonant contribution to $P_{\vec{q}}(\omega)$ from Eq. (32). The influence of the resonant contribution is apparent in Fig. 2, however the $\ell = 1$ non-resonant term is also very big.

In Fig. 3, we plot a hypothetical line shape $L_{\vec{q}}^R(\omega)$, obtained neglecting non-resonant contributions to $P_{\vec{q}}(\omega)$, and in Fig. 4 we plot the line shape given by Eq. (35), with non-resonant terms included. In both figures we show the line shape for several values of the magnetic field H . It is clear from these figures that the effect of the non-resonant term is to shift the strongly distorted lines to higher field regions, which is equivalent to a shift in the phonon frequency ω_0 .

To give an idea of the strong angular dependence of the spectrum, we show in Fig. 5 the line shape as a function of ϕ . This angular dependence is the result of an enhancement of the phonon relaxation with increasing q_{\perp} , the momentum transfer perpendicular to the magnetic field. On the other hand, we note that the width of the frequency range for which $\gamma_{\vec{q}}(\omega)$ is different from zero depends on q_z , the component of the phonon momentum parallel to the magnetic field. Therefore a delicate balance is needed for the contribution from $\gamma_{\vec{q}}(\omega)$ to the line shape to be important throughout a reasonable range of frequency.

Finally we introduce amplitude effects, calculated in section IV. In Fig. 6 we plot $N_q^{\prime}(\omega)$ and $N_q^{\prime\prime}(\omega)$, real and imaginary parts of the scattering amplitude, as a function of frequency for several values of the electron lifetime. Here we approximate the electron damping $\Gamma_{n,n+l}$ by Γ_e for the levels involved in the calculations.

In Fig. 7 we plot the differential extinction coefficient given by Eq. (26) as a function of frequency for two different values of ω_c . The line corresponding to $\omega_c/\omega_0 = 0.55$ has a very complex structure because the phonon mode interacts with a continuum of electronic excitations and for this value of ω_c the renormalized phonon frequency lies within the continuum. For $\omega_c/\omega_0 = 0.45$, on the other hand, the renormalized phonon frequency does not lie within the continuum and we clearly see a strong line around the renormalized phonon frequency and a small structure in a frequency region corresponding to the electronic excitations. This spectrum is very characteristic of a hybrid mode. We estimate the extinction coefficient to be approximately $8 \times 10^{-9} \text{ cm}^{-1}$ which is within the detectable experimental range.

In computing the curves of Figs. 3, 4, 5 and 7 we have added phenomenologically a constant damping $\gamma_0 = 0.01 \omega_0$, to the frequency dependent $\gamma_q^{\prime}(\omega)$ to take care of contributions to the phonon lifetime coming from other processes not included in this calculation.

VI - CONCLUDING REMARKS

We have considered the effect, on the Raman spectrum of a type-n semiconductor, of the hybridization of the LO phonon and cyclotron modes through the Fröhlich interaction. Neglecting the

lifetime of the electron states we have related the extinction coefficient to the double-time Green's function formalism⁽¹⁷⁾. We have calculated the phonon Green's function for an electron-phonon system coupled via the Fröhlich interaction and in the presence of a constant magnetic field. We give special attention to magnetic field values such that the LO phonon frequency is an integral multiple of the cyclotron frequency.

Genkin and Zil'berberg⁽⁶⁾ have shown that in these field regions, the process (a) of Fig. 1 is resonant and may dominate over process (b). These authors neglect the k_z dependent term in the electron energy and made no attempt to calculate the effect of mode hybridization which may be very important under these resonant conditions.

Our results show the importance of including the k_z dependence in the electron energy, not only because $k_{zF}^{(n)}$ may be reasonably big and the approximation of neglecting k_z may be a poor one in some cases, but because it is vital for the existence of hybridization effects on the line shape. These effects come from the interaction of the LO phonon mode with a continuum of electronic excitations. If we neglect k_z this continuum is destroyed. Furthermore, Genkin and Zil'berberg consider the case of carrier concentrations such that the Fermi energy is less than $(3/2) \hbar\omega_c$. This is equivalent, in our work to consider only the case where $n_0 = 0$, which in general is very restrictive. Neglecting k_z in the energy denominators of Eq. (21) and taking $n_0 = 0$, therefore retaining only one term in the sum over n , we retrieve the results of Genkin and Zil'berberg as is expected.

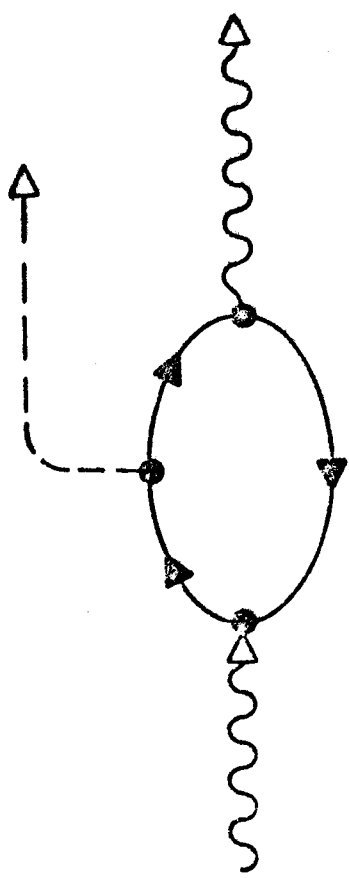
REFERENCES

1. J.J. Hopfield and C.H. Henry, Phys. Rev. Lett. 15, 964 (1965).
2. A. Mooradian and G.B. Wright, Phys. Rev. Lett. 16, 999 (1966).
3. C.K.N. Patel and R.E. Slusher, Phys. Rev. Lett. 22, 282 (1969).
4. C.A. Argüelo, D.L. Rousseau and S.P.S. Porto, Phys. Rev. 181 , 1351 (1969).
5. P.A. Wolff, Phys. Rev. Lett. 16, 225 (1966); Phys. Rev. 171 , 436 (1968).
6. G.M. Genkin and V.V. Zil'berberg, Fizika Tverdogo Tela 11, 1812 (1969) [English Translation: Soviet Phys. - Solid State 11 , 1465 (1970)] .
7. R. Luzzi, Prog. Theor. Phys. 47, 13 (1972).
8. R.E. Slusher, C.K.N. Patel and P.A. Fleury, Phys. Rev. Lett. 18, 77 (1967); C.K.N. Patel and R.E. Slusher, Phys. Rev. 167 , 413 (1968).
9. Harper ⁽¹⁰⁾ has also discussed the possibility of cyclotron Raman scattering induced by polaron interaction, i.e. when anharmonicity of the Landau levels in semiconductors with parabolic conduction band edge is provided by the electron-phonon interaction. However, this contribution to the scattering cross section is also very small.
10. P.G. Harper, Phys. Rev. 178, 1229 (1969).
11. G.P. Vella-Coleiro, Phys. Rev. Lett. 23, 697 (1969).
12. H. Fröhlich, Adv. in Phys. 3, 325 (1954).
13. L.D. Landau and E.M. Lifshitz, "Quantum Mechanics", (Pergamon Press, London, 1958) p. 474.
14. A.L. Fetter and J.D. Walecka, "Quantum Theory of Many-Particle

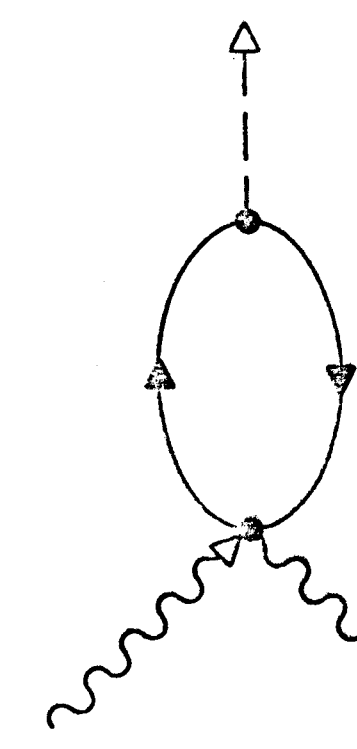
- Systems" (McGraw-Hill, New York, 1971) p. 70.
15. L.D. Landau and E.M. Lifshitz, "Electrodynamics of Continuous Media" (Pergamon Press, Oxford, 1960) p. 386.
 16. L. van Hove, Phys. Rev. 95, 249 (1954).
 17. D.N. Zubarev, Usp. Fiz. Nauk 71, 71 (1960) |English translation: Soviet Physics - Uspekhi 3, 320 (1960)|.
 18. A.Ya. Blank and E.A. Kaner, Zh. Eksp. Teor. Fiz. 30, 1058 (1956) |English translation: Soviet Physics - JETP 23, 673 (1966)|.
 19. A.S. Davydov, "Quantum Mechanics" (Addison Wesley, Reading, 1964), p. 309.

FIGURE CAPTIONS

- Figure 1. Processes contributing to the phonon scattering.
- Figure 2. Real, $P(\omega)$, and imaginary, $\gamma(\omega)$, parts of the polarization operator $\hat{P}(\omega)$. $P^R(\omega)$ is defined in the text.
- Figure 3. The line-shape, $L^R(\omega)$, resulting when only the resonant $P^R(\omega)$ contribution is included.
- Figure 4. The line-shape function $L(\omega)$ for several values of the magnetic field.
- Figure 5. The line-shape $L(\omega)$ for several values of the angle between phonon propagation and magnetic field.
- Figure 6. The real, $N'(\omega)$, and imaginary, $N''(\omega)$, parts of the scattering amplitude.
- Figure 7. The differential extinction coefficient for two different values of the magnetic field.



(a)



(b)

—▶ electron - - -▶ electron wavy▶ photon wavy▶ phonon

FIG. 1

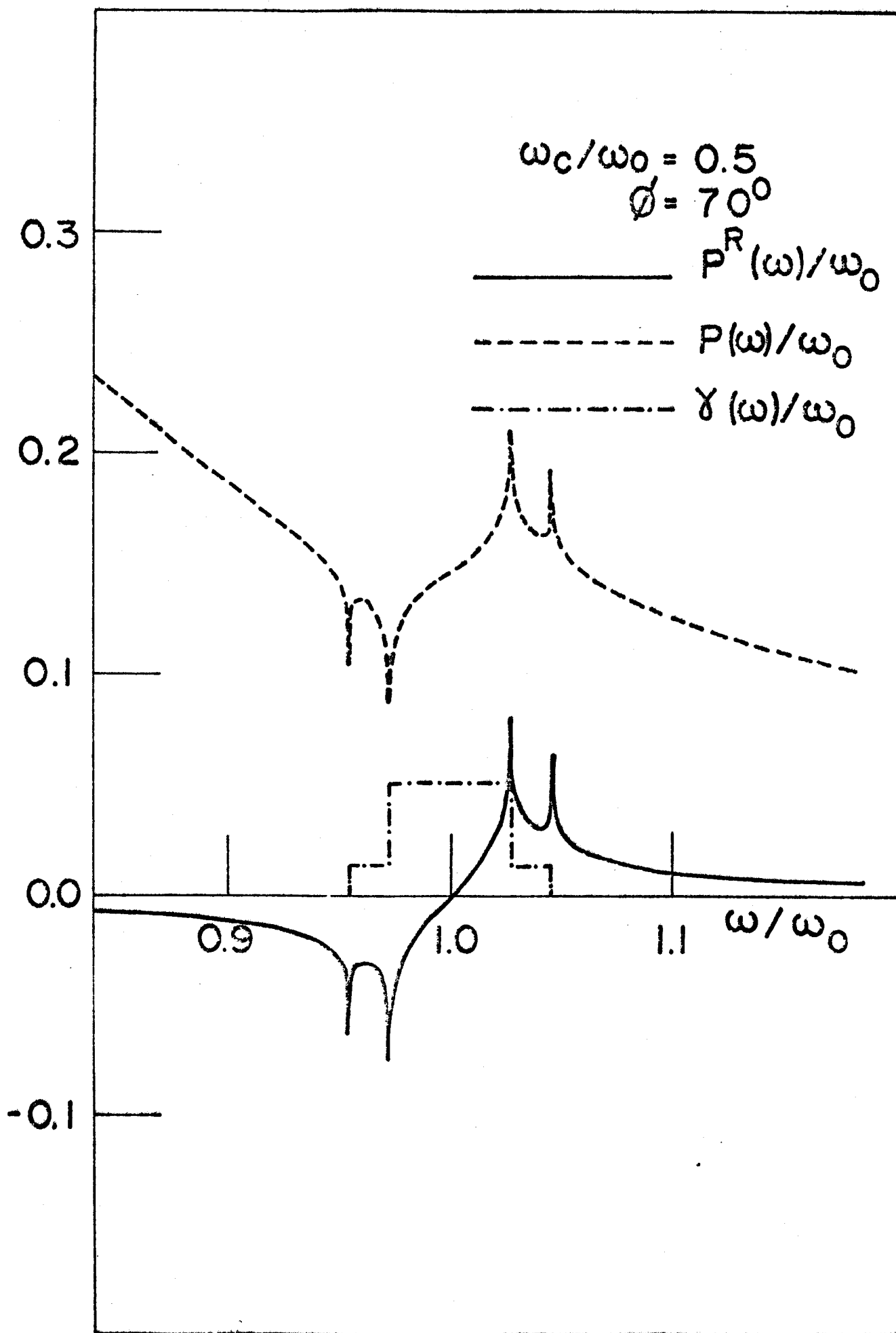


FIG. 2

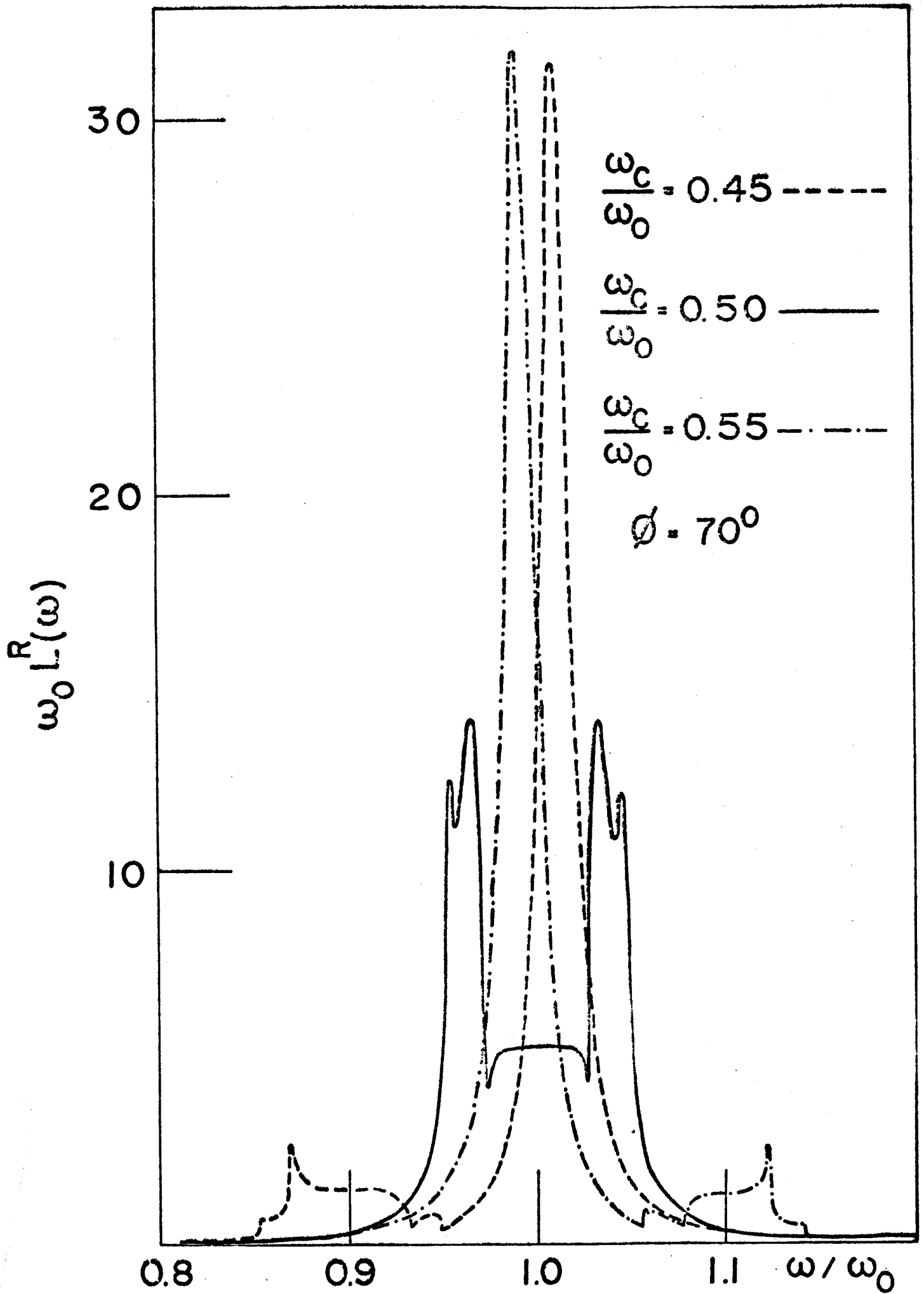


FIG. 3

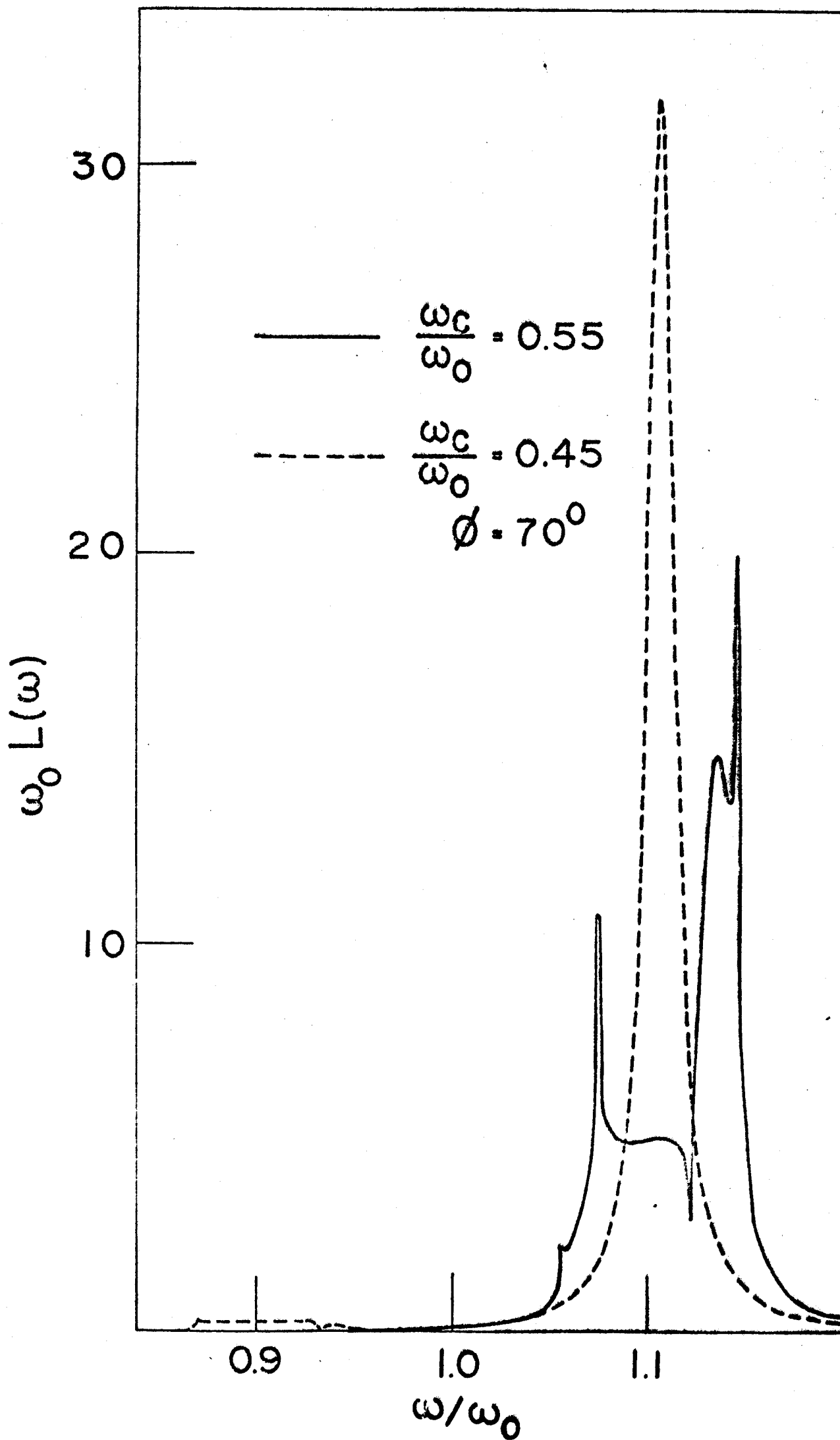


FIG. 4

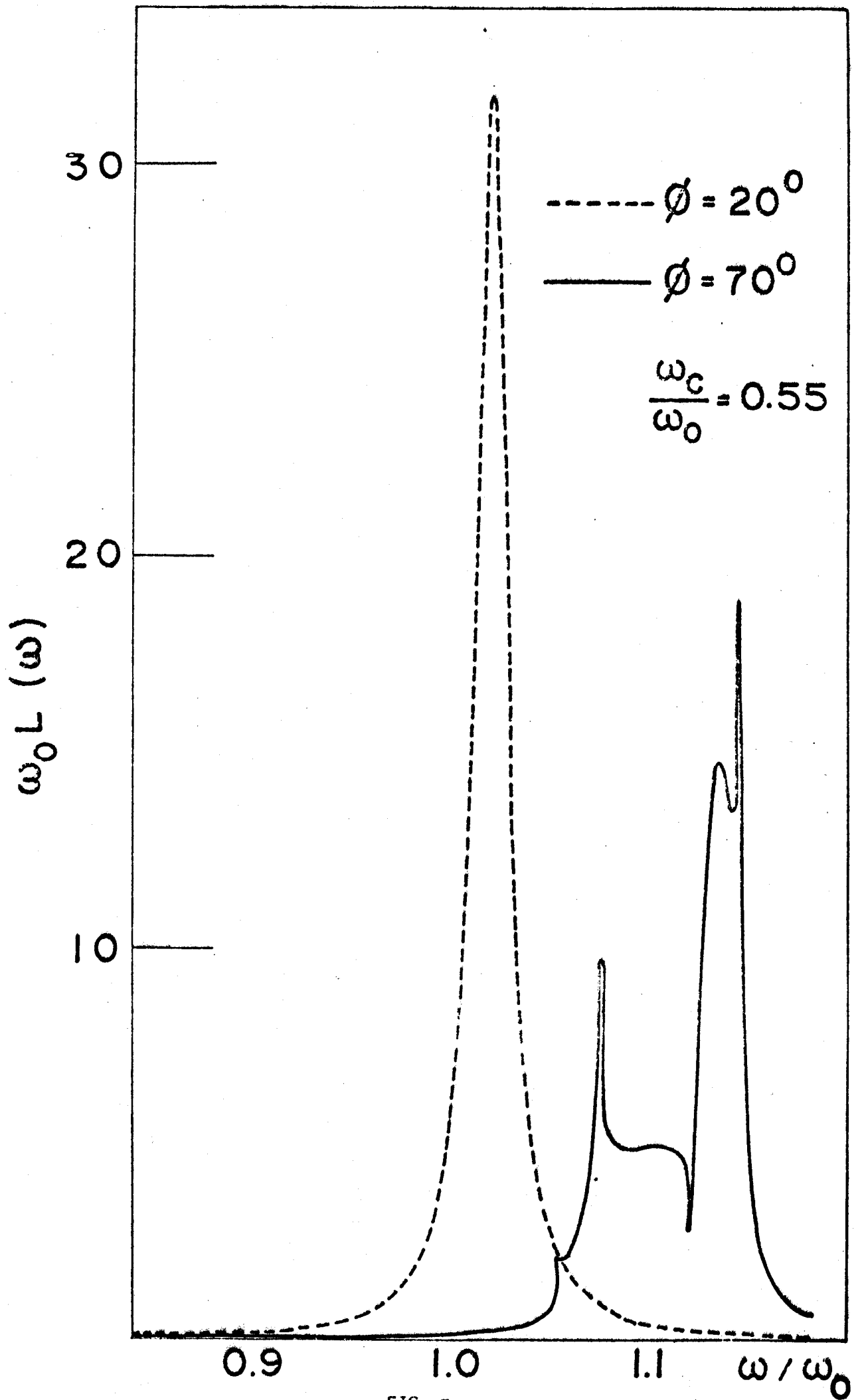


FIG. 5

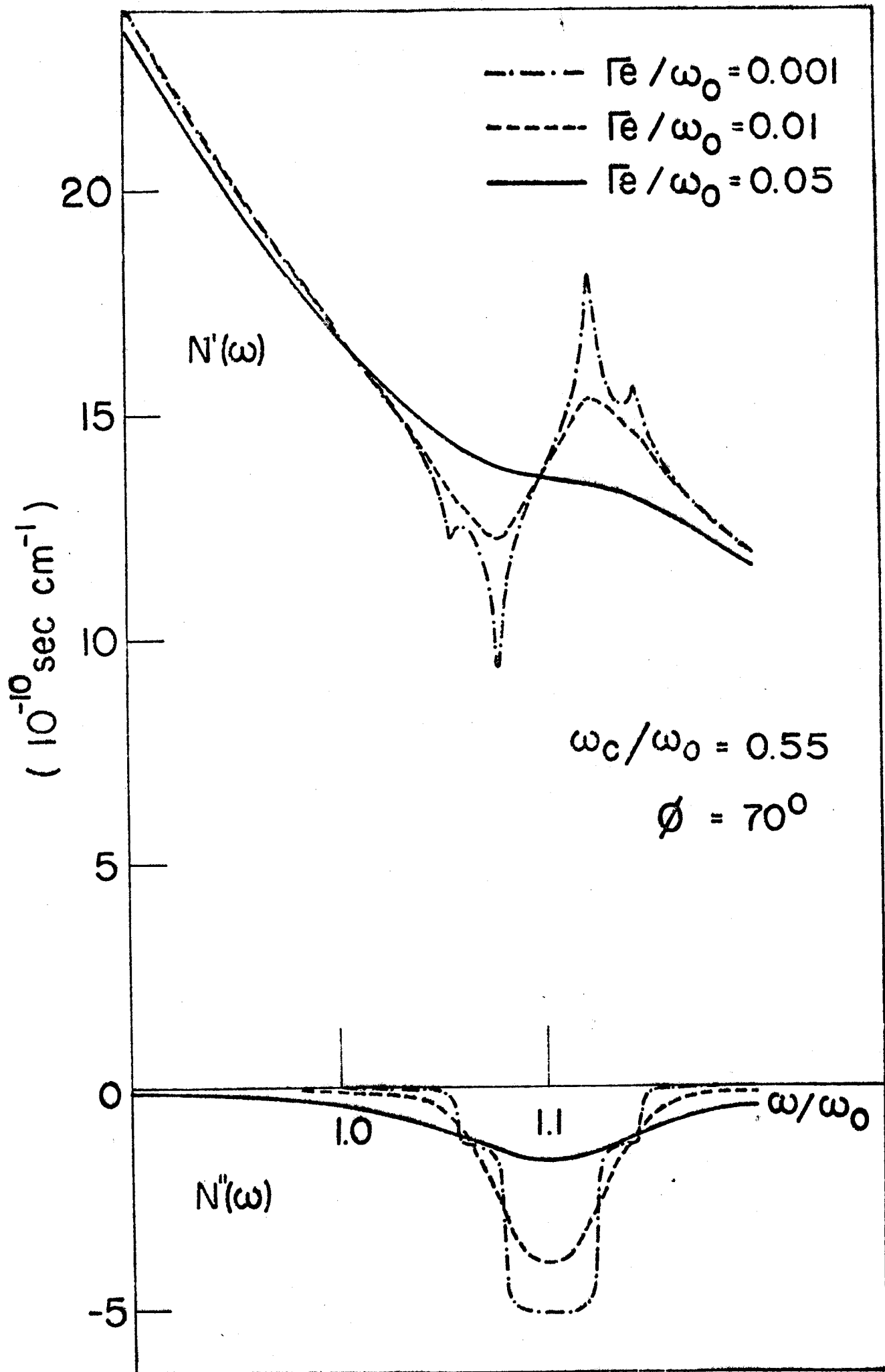


FIG. 6

Differential Extinction Coefficient (10^{-21} sec cm^{-1})

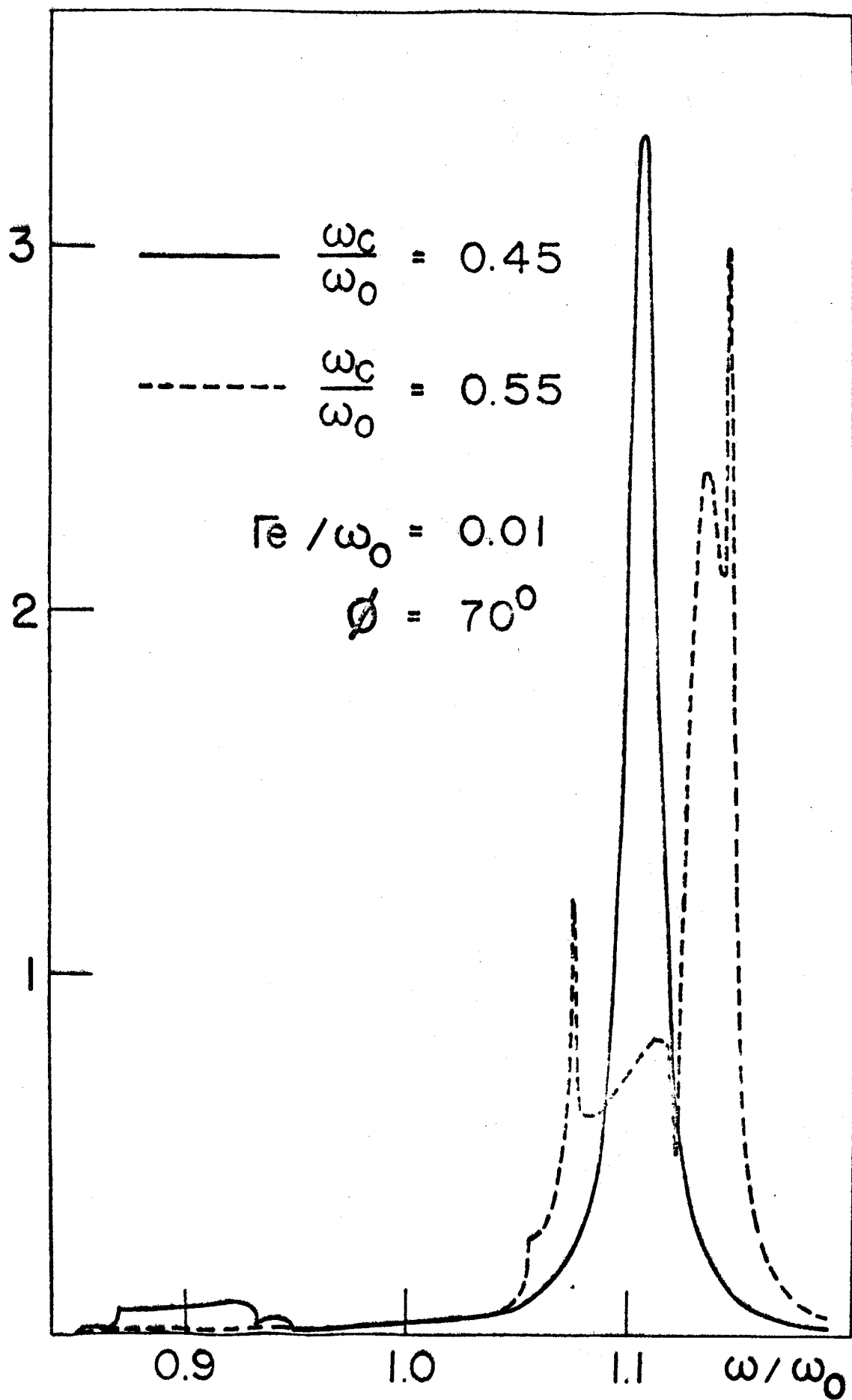


FIG. 7